Published in final edited form as:
J Biosci Bioeng. 2010 October ; 110(4): 459–470. doi:10.1016/j.jbiosc.2010.04.004.

Effects of Substrate Stiffness and Cell Density on Primary Hippocampal Cultures

Michelle L. Previtera[1,3], **Christopher G. Langhammer**[2,3], and **Bonnie L. Firestein**[3,4,*]

[1]Molecular Biosciences Graduate Program, Rutgers, the State University of New Jersey, 604 Allison Road, Piscataway, New Jersey 08854-8082; USA.

[2]Biomedical Engineering Graduate Program, Rutgers, the State University of New Jersey, 604 Allison Road, Piscataway, New Jersey 08854-8082; USA.

[3]Department of Cell Biology and Neuroscience, Rutgers, the State University of New Jersey, 604 Allison Road, Piscataway, New Jersey 08854-8082; USA.

[4]Department of Biomedical Engineering, Rutgers, the State University of New Jersey, 604 Allison Road, Piscataway, New Jersey 08854-8082; USA.

Abstract

Previous studies have shown that dendrites are influenced by substrate stiffness when neurons are plated in either pure or mixed cultures. However, because substrate rigidity can also affect other aspects of culture development known to impact dendrite branching, such as overall cell number, it is unclear whether substrate stiffness exerts a direct or indirect affect on dendrite morphology. In this study, we determine whether substrate stiffness plays a critical role in regulating dendrite branching independent of cell number. We plated primary mixed hippocampal cultures on soft and stiff gels, with Young's moduli of 1 kPa and 7 kPa, respectively. We found that neurons plated on stiffer substrates showed increased branching relative to neurons grown on softer substrates at the same cell number. On the stiff gels, we also observed a cell number-dependent effect, in which increasing initial plating density decreased dendrite branching This change correlates with an increase in extracellular glutamate. We concluded that both cell number and substrate stiffness play roles in determining dendrite branching, and that the two effects are independent of one another.

Keywords

dendrite branching; dendrite arborization; hydrogel; astrocytes; cellular adhesion; astrocytes; glutamate

INTRODUCTION

A century ago, Ramon y Cajal determined that thorough examination of neuronal morphology, including characterization of the dendritic arbor, would help to better elucidate overall nervous system function. Dendrite branching is a highly dynamic process and determines the role that

*To whom correspondence should be addressed: firestein@biology.rutgers.edu; Phone: 732-445-8045; Fax: 732-445-5870.

a neuron will play in a neuronal circuit (1–3). Proper development of the dendritic arbor is important for normal nervous system function, and abnormalities in branching patterns occur in a number of cognitive disorders, including Alzheimer's disease, Down syndrome, autism, Rett syndrome, and schizophrenia (4–6).

The development of the dendritic arbor is a multi-stage process and can be observed using cultured dissociated rat hippocampal neurons. At initial plating, neurons form lamellipodia that adhere to the substrate on which they are plated (stage 1)(7). Next, primary dendrites extend from the soma from 1 day *in vitro* (DIV) until at least 10 DIV (stages 2–4) (7). Higher order branches then extend from the primary dendrites from 6 DIV until 12 DIV (stage 4) (7,8). Soon after, a maturation process occurs from 12 DIV until 21 DIV by permitting spine formation and pruning of some of the primary and secondary dendrites (stage 5) (7).

The stages of dendrite development are influenced by numerous intrinsic and extrinsic factors (9). Recently, it has been shown by a number of groups, including our own, that the molecular mechanisms that underlie the trafficking of receptors and signaling elements to postsynaptic sites also help to shape the dendritic arbor (10,11). In our studies and in previously published work, it has been shown that as cells are plated on increased substrate stiffness, an increase in cell density occurs due to differences in adhesion and growth of different cell types (12–14). Furthermore, cell density could affect dendrite morphology due to variations in cell-cell contact, synaptic density, and the global concentration of extrinsic factors (7,10,15–25). Thus, it is of importance to examine whether cell density in mixed cultures plays a role in determining the dendrite branching phenotypes seen in neurons plated on hydrogels of varying rigidities. In the current study, we examine the effects of substrate stiffness on dendrite morphology when primary mixed hippocampal cultures were grown on compliant substrates. We also examine the effects of cell density on dendrite branching parameters.

In this study, we plated primary mixed cultures of hippocampal cells on polyacrylamide (PA) gels to assess the effects of varying cell densities on two different substrate rigidities. PA gels are used in this study because we are able to make substrates with varying rigidities by varying the percentage of the crosslinker, bis-acrylamide (12,26,27). In addition, varying the percentage of crosslinker does not vary the pore size or amount of adhesion sites on the gels (12,26–28). We observed that substrate stiffness plays a larger role in determining branching patterns than does cell density. However, cell density does indeed influence dendrite branching on stiff substrates.

MATERIALS AND METHODS

Antibodies

Neurons were immunostained using anti-MAP2 (Chemicon, Temecula, CA, USA), mature astocytes were immunostained using anti-GFAP (Chemicon, Temecula, CA, USA), and immature astrocytes were immunostained using anti-vimentin (Chemicon, Temecula, CA, USA). Microglia were immunostained using anti-OX42, and oligodendrocytes were immunostained using anti-CNPase (Chemicon, Temecula, CA, USA). Nuclei were stained using 4',6-diamidino-2-phenylindole (DAPI) or Hoechst dye.

PA Gel Preparation

PA gels were made as previously described (12,26). Briefly, gels were composed of 7.5% acrylamide and 0.02, 0.03, 0.1, or 0.6% *N, N8*-methylene-bis-acrylamide, for varying rigidities, in 50 mM HEPES, pH 8.2 (HEPES). 12 mm round glass coverslips were treated with aminopropyl trimethoxy sulfate for 3 mins followed by 0.5% glutaraldehyde for 30 mins. Gels were polymerized on coverslips with N, N, N9, N9-tetramethylethylenediamine (TEMED) and

ammonium persulfate and a Rainx (Houston, TX) treated coverslip was place on top to ensure an even topology. Gels were composed of 7.5% acrylamide and 0.02, 0.03, 0.1, or 0.6% *N*, *N8*-methylene-bis-acrylamide, for varying rigidities, in 50 mM HEPES, pH 8.2. Gels were polymerized on 12 mm round glass coverslips with N, N, N9, N9-tetramethylethylenediamine (TEMED) and ammonium persulfate. Next, gels were functionalized by UV irradiation of Sulfo-SANPAH in HEPES. Gels were placed in 12 well plates, and poly-D-Lysine (PDL; 0.2 mg/ml in HEPES) was placed onto the gels and inside of the wells for 30–60 minutes at 37° C. For PDL coating studies, PDL was conjugated to Oregon Green using a FluoReporter Oregon Green 488 Protein Labeling Kit according to the manufacturer's instructions with modification (Invitrogen, Carlsbad, CA, USA). PDL conjugated to Oregon Green was not purified through a column. Gels were equilibrated for at least 30 minutes in 12 well plates with Neurobasal media, supplemented with B27, penicillin, streptomycin, L-glutamine with 27 μM 2-mercaptoethanol or Glutamax (all from Invitrogen, Carlsbad, CA, USA), or with 50 mM HEPES, pH 8.2.

Mechanical Testing

Cylindrical samples of polyacrylamide gels were prepared and placed in Neurobasal media at 37°C with 5% CO_2 for 16 – 48 hours. A compression testing machine with a Mark-10 EG 025 series digital force gauge (Johnson Scales, West Caldwell, NJ, USA) and a strain gauge was used to compress the gels. The Young's modulus (stiffness) was calculated using a linear trend line of the load deflection curve. Compression was less than 10% of the original height of the sample. Linear elastic theory was applicable because the graph was linear.

Primary Mixed Hippocampal Culture

Neuronal cultures were prepared from hippocampi of E18 rat embryos as previously described (8,11,29). The hippocampi were dissociated by mechanical trituration. Cells were plated onto the gels at the indicated initial densities. Cultures were maintained in supplemented Neurobasal media as described under the section PA Gel Preparation.

Transfection

Neurons were transfected on 7 or 8 DIV with cDNA encoding GFP using the calcium phosphate method. This was performed for dendrite visualization (30–33). Briefly, 75 μl of 2X HeBS (pH 7.1; 274 mM NaCl, 10 mM KCl, 1.4 mM $Na_2HPO_4 \cdot 7H_2O$, 15 mM dextrose, and 42 mM HEPES) was mixed with 75 μl of a solution containing 15 μg of DNA and 0.25 M $CaCl_2$. This mixture was incubated for 25 minutes in the dark at room temperature. Next, 60–100 μl of the mixture was dropped into each well containing 1 ml of Neurobasal media supplemented with B27 only. The solution was allowed to precipitate for 30–45 minutes with the cells in the tissue culture incubator. Media containing precipitate was removed and replaced with the original supplemented Neurobasal media plus 15% fresh supplemented Neurobasal media.

Immunocytochemistry

Cultures were fixed with 4% paraformaldehyde in phosphate-buffered saline (PBS) for 30 minutes at 37°C at indicated time points. Neurons were permeabilized in blocking solution (5% normal goat serum, 0.02% sodium azide, and 0.1% Triton X-100 in PBS). Neurons were immunostained using a 1:500 dilution of the indicated antibody for 1–2 hours at room temperature or overnight at 4°C and then incubated for 1–2 hours with a secondary antibody conjugated to fluorophore (Jackson ImmunoResearch, West Grove, PA, USA).

Dendrite Analysis and Imaging

Neurons expressing GFP were imaged in the GFP channel at 200x using an Olympus Optical IX50 microscope (Tokyo, Japan) with a Cooke Sensicam CCD cooled camera, fluorescence

imaging system, and ImagePro software (MediaCybernetics, Silver Spring, MD). A HQ4080/20x filter set was used to excite GFP-expressing cells with an excitation wavelength of 465–492 nm (Chroma Technology Corp., Rockingham, VT, USA). Pictures were taken only where neurons or astroglia adhered to the gels. For branching studies, neurons were selected only if transfected to prevent bias. No neurons were discarded from analysis. Based on confirmation with MAP2 immunostaining that neurons can be selected using morphological characteristics, pictures of glia were not taken. Representative images were inverted to black cells on a white background to show branching details.

In the first stage of dendrite analysis, the semi-automated tools available through the NeuronJ (34) plugin to ImageJ (NIH, Bethesda, MD, USA) were used to define the locations of all neurites. The longest neurite was tagged as the axon and was eliminated from tracings. The use of this computer-assisted digitization process has been shown to be at least as accurate as fully manual and fully automated digitization of neuronal morphology *in vitro* (34,35). Custom scripts written in MATLAB (MathWorks, Natick, MA, USA) were used to transfer the data from NeuronJ to 'SWC' format, a file structure used for storing neuronal morphology data (36,37). In the second stage, NeuronStudio was used to define the pattern of connectivity between dendrites, without disrupting their locations as identified in the first step (38). These two steps fully and accurately define the structure of each cell's dendrite arbor through a computer-assisted tracing process, and encode it in a digital format. Digital formats were checked against original pictures and manual counting to assure proper functioning of the automated portion of the program. Using these digitized dendrite arbors, a second set of custom MATLAB scripts were used to calculate the following metrics: number of primary dendrites, number of secondary dendrites, number of branch points per cell, number of terminal dendrite points per cell, and Sholl analysis performed with a 9.3 μm ring interval for the first ring and then 6 μm for successive ring intervals. Sholl analysis is performed by drawing concentric circles around the cell body and counting the intersections (i.e. dendrites) that cross each circle. The number of intersections is graphed versus distance from the cell body to give a curve that describes the shape of the dendritic arbor. Data were exported to Excel to facilitate statistical analysis in other analytical platforms (Instat Software, San Diego, CA, USA). The experimenter was blinded to condition during all digitization and statistical analysis. Dendrites were labeled as proximal (1–63 μm from the cell body), intermediate (64–123 μm from the cell body), and distal (124–183 μm from the cell body). Statistics were not performed for intersections >183 μm from the cell body because of interference by neighboring neurons and limitations on imaging. As stated above, axons were excluded from analyses.

Glutamate Assay

Media was collected and either used fresh or snap frozen by liquid nitrogen and stored at −80° C prior to the assay (Sigma, St, Louis, MO, USA). The glutamate assay was performed according to the manufacturer's instructions with modification. 500 μl of total reaction was used with 123 μl of media. The reaction was allowed to proceed for 3 hours.

Statistical analysis

Only data sets that included appropriate controls were included in analyses. GraphPad Instat Software (San Diego, CA, USA) was used to calculate statistics. For data averaged across all experiments with more than two conditions, one-way ANOVA test was performed followed by the appropriate *post hoc* test. If the data did not follow a Gaussian distribution or if Bartlett's test suggested a significant difference among standard deviations, Kruskal-Wallis, a non-parametric test, was performed followed by the appropriate *post hoc* test. For data averaged across all experiments with only two conditions, a Student's t-test was performed. If the data did not follow a Gaussian distribution, a Mann-Whitney test, a non-parametric test, was performed. For data averaged within each experiment with more than one condition, a repeated

one-way ANOVA test was performed followed by the appropriate *post hoc* test. If repeated one-way ANOVA was not effective, one-way ANOVA was performed, and the experimenter followed the instructions above. For data averaged within each trial with two conditions, a paired t-test was performed. If a paired t-test was not effective, a Student's t-test was performed, and the experimenter followed the instructions above. These statistics are standards in the field of biology (8,11,39,40).

RESULTS

Substrate stiffness affects cell number

We first determined the number and densities of specific cell types on various gel rigidities. We plated primary mixed cultures of hippocampal cells on gels ranging from 0.02 to 0.6% bis-acrylamide at an initial plating density of approximately 60,000 cells/cm^2. Previously published work has shown that as the percentage of bis-acrylamide increases, the stiffness of the gel increases (14,26). Cultures were fixed on 12 DIV and immunostained with antibodies to various cell-type specific markers. All positively stained cells observed in the field were counted. We observed that as the percent of bis-acylamide increased from 0.03% to 0.1%, the number of total cells increased (Figure 1A, inset). No further increase in cell number was seen when cells were plated on gels of 0.6% bis-acrylamide. We then analyzed specific cell populations and saw that the number of neurons (MAP2-positive cells) and mature astrocytes (GFAP-positive cells) increased while the number of immature astrocytes (vimentin-positive cells) did not change as stiffness increased (Figure 1 A and B). We also counted OX42- and CNPase-positive cells to determine the number of microglia and oligodendrocytes, respectively, on the various compliant substrates. Very few, if any, of these cell types were present (data not shown).

It has been reported that gel composition can greatly influence cell number (41). To test if variations in PDL coating influence cell number on polyacrylamide gels of varying stiffnesses, we measured the amount of PDL adsorbed onto and retained by 0.02–0.6% polyacrylamide gels (Figure 1 C). Gels were coated with 0.2 mg/ml of PDL conjugated to Oregon Green. Five images of each gel were taken at 200X in the GFP channel at the same exposure time. The average pixel intensity was measured for each picture. Prior to PDL coating, pictures were taken at the same exposure time with gels functionalized with only Sulfo-SANPAH to evaluate if Sulfo-SANPAH contributes to background fluorescence. Sulfo-SANPAH intensity remained unchanged among gel conditions (data not shown). As stiffness increased, the amount of PDL decreased. Since increased PDL should result in increased cellular adhesion, the fact that the gels with the lowest amount of PDL showed the highest number of cells strongly suggests that stiffness influences cell number on the various gels rather than the amount of PDL retained by the gels.

We then asked whether the differences in cell number were due to differences in cell attachment during plating. Cells were plated onto gels at an initial density of approximately 60,000 cells/cm^2, the density that we have previously plated our neurons on glass (8,11,39,40). Neurons were fixed at 24 and 48 hours after plating and immunostained for MAP2. We also immunostained for GFAP, but we found that these time points were too early in culture to observe mature astrocytes. At both 24 and 48 hours after plating, we observed the same trend in the number of neurons found on the gels as we observed on 12 DIV. We found that as the percentage of bis-acrylamide increased, the number of neurons found on the gels increased (Figure 2 A–D). Thus, the increase in the number of neurons seen on stiffer gels may be due, at least in part, to increased cell attachment on stiffer substrates during the initial plating. Cultures contain primary hippocampal neurons that are postmitotic; thus, cell division does not contribute to the differences in cell number due to an increase in substrate stiffness.

To ensure that gel stiffness increases as percent bis-acrylamide increases, we performed compression testing on 0.02% and 0.1% polyacrylamide gels. These gels were selected because they were used in the branching and plating studies performed below. Young's moduli of soft and stiff gels were determined to be 1 kPa (SEM±0.08) and 7 kPa (SEM±0.47; Figure S1).

Next, we wanted to observe whether increasing (approximately 80,000 and 100,000 cells/cm^2) or decreasing (approximately 50,000 cells/cm^2) the initial plating density leads to changes in the number of cells on either soft (1 kPa) or stiff (7 kPa) gels when compared to the original plating density of 60,000 cells/cm^2. We attempted to plate at a lower initial density of 30,000 cells/cm^2, but we obtained little cell attachment, particularly on the 1 kPa (soft) hydrogels (data not shown). As the initial plating density increased, the total number of cells did not change for soft or stiff gels (Figure 3 A and B inset). However, on soft gels, the number of neurons and mature astrocytes, but not immature astrocytes, increased with an increase in the initial plating density (Figure 3 A, Figure S2). Furthermore, the number of neurons and astrocytes, both mature and immature, increased on stiff gels with an increase in the initial plating density (Figure 3 B, Figure S2). The discrepancy between the increased number of neurons and astrocytes and the unchanged number of total cells on soft and hard gels could be due to the presence of other cell types that influence total cell count, such as endothelial cells. These findings demonstrate that the gels show a higher number of neurons and astrocytes as the plating density is increased.

When gels with the same initial plating densities were compared on 12 DIV, cells did not always attach better to stiff gels than to soft gels. When cells were plated at an initial density of 50,000 cells/cm^2, the same numbers of neurons and astrocytes were found on soft and stiff gels (Figure 3 C and Figure S2). However, when cells were plated at an initial density of 80,000 cells/cm^2, more mature and immature astrocytes, but not neurons, were found on stiff gels than on soft gels (Figure 3 D and Figure S2). Moreover, when cells were plated at an initial density of 100,000 cells/cm^2, only mature astrocytes were found at higher numbers on stiff gels than on soft gels (Figure 3 E and Figure S2). These data demonstrate that the initial plating density affects the number of specific cell types that are found on soft and stiff gels.

Substrate stiffness does not affect astrocyte/neuron ratio

Since there is a difference in the number of astrocytes on soft and stiff gels but no difference in the number of neurons, we asked whether there was a difference in the astrocyte/neuron ratio at different plating densities. For these experiments, we double-immunostained for GFAP or vimentin and MAP2 and took images of the two subtypes of cells in the same field. The ratio of mature astrocytes/neurons and immature astrocytes/neurons on soft or stiff gels did not change as plating density increased (Figure S3 A and B, respectively). At equivalent plating densities, the ratio of mature astrocytes/neurons and immature astrocytes/neurons did not change between soft and stiff gels (Figure S3 C and D, respectively).

Next, we compared the number of cells found on soft gels plated with 100,000 cells/cm^2 and the stiff gels plated with 50,000 cells/cm^2 to see whether, at different initial plating densities, both the soft and stiff gels would have the same number of neurons and astrocytes as well as the same ratio of astrocytes/neurons. We found that soft gels plated with 100,000 cells/cm^2 and stiff gels plated with 50,000 cells/cm^2 had the same number and ratio of cells (Figure 3 F, Figure S2, and Figure S3 A and B insets). Thus, final cell densities and ratio of astrocytes/neurons are the same for soft gels plated with 100,000 cells/cm^2 and stiff gels plated with 50,000 cells/cm^2.

Cell density affects dendrite branching differently when cells are plated on soft versus stiff gels

Since cell density affects dendrite morphology (7,10,15–25), we assessed dendrite morphology in neurons cultured on our gels. Cells were plated at initial densities of 50,000, 80,000 and 100,000 cells/cm^2 on either soft or stiff gels and were fixed on 12 DIV. At equivalent initial plating densities, neurons plated on stiff gels consistently had more primary and secondary dendrites than neurons plated on soft gels (Figure 4 A, B, E).

To fully understand how stiffness and cell density affect dendritogenesis, we examined additional branching parameters, including the number of branch points and the number of terminal points. As expected, dendrites of neurons plated on the stiffer gels had more terminal points than those of neurons grown on the soft gels at all plating densities (Figure 4 C and E). Similar to terminal point number, dendrites of neurons plated on stiff gels had more branch points than dendrites of neurons grown on soft gels at all plating densities (Figure 4 D and E).

Next, we observed if branching parameters changed at the various plating densities on soft gels. The number of primary and secondary dendrites, terminal points, and branch points in neurons plated on soft gels did not change as the plating density increased (Figure 5 A and C). In contrast, neurons plated on stiff gels showed a decrease in the number of primary and secondary dendrites as the initial plating density was increased (Figure 5 B). In addition, the number of terminal points decreased as the plating density was increased for neurons grown on stiff gels (Figure 5 D). The number of branch points on dendrites did not change as the initial plating density was increased on soft or stiff gels (Figure 5 D). These results agree with the data for primary and secondary dendrite number. Thus, cell density affects dendrite number when neurons are plated on stiff but not soft gels.

Next, we assessed whether differences in cell densities contribute to changes in branching parameters or whether the changes in branching are due solely to variations in substrate stiffness. We compared cells plated at the highest density (100,000 cells/cm^2) on soft gels with cells plated at the lowest density (50,000 cells/cm^2) on stiff gels because they have equivalent numbers of neurons and astrocytes (Figure S3 F). At equivalent cell numbers, neurons plated on stiff gels had more primary and secondary dendrites. Moreover, cells plated at an initial density of 50,000 cells/cm^2 on stiff and soft gels also had the equivalent number of cells and ratio of astrocytes/neurons, and neurons on soft gels had fewer dendrites and branch points (Figures 3–5, Figure S3). Thus, our experiments show that substrate stiffness, but not cell density, affects dendrite patterning.

Stiffness and cell density affect dendrite patterning

We then assessed the role of substrate stiffness and cell density on overall dendrite branching patterns. Sholl analysis was performed by drawing multiple concentric circles around the cell body at a fixed distance, in this case, 9.3 μm, and counting the number of dendrites that intersect each circle (Figure 6 A).

To determine if dendrite branching patterns differ between neurons plated on soft or stiff gels when the initial plating densities are equivalent, we performed Sholl analysis on the neurons plated on both soft and stiff gels at each plating density. There were more proximal and intermediate dendrite intersections when neurons were plated on stiff gels when compared to neurons on soft gels for all initial plating densities (Figure 6 B–D). These data coincide with the trends that we observed for dendrite number, terminal point, and branch point numbers.

To assess whether dendrite branching patterns differ when cells are plated at different densities on a single substrate stiffness, we performed Sholl analysis on the neurons plated at each density for each substrate stiffness. Sholl curves from the analysis of dendrites of neurons plated on

soft gels were the same regardless of the initial plating density (Figure 7 A). However, there was a decrease in the number of proximal dendrite intersections of neurons grown on hard gels as the initial plating densities increased (Figure 7 B). These data coincide with the trends we observed for dendrite number, terminal point, and branch point numbers. These data suggest that cell density plays a role in shaping the dendritic arbor close to the cell body on stiff, but not soft, gels.

Finally, we assessed if branching parameters of neurons cultured on soft and stiff gels are influenced by differences in cell density. We performed Sholl analysis on the neurons plated on soft gels with an initial plating density of 100,000 cells/cm^2 and on the neurons plated on stiff gels with an initial plating density of 50,000 cells/cm^2 as these two experimental groups have equivalent numbers of both neurons and astrocytes and equivalent cell ratios (Figure S3 F). There were a greater number of both proximal and intermediate dendrite intersections in neurons that were plated on stiff gels as compared to neurons plated on soft gels that had the equivalent final cell density (Figure 7 C). Neurons cultured on stiff gels had more proximal intersection than those cultured on soft gels (Figure 6 A). Thus, regardless of initial plating density or final cell number on the gels, there are differences in the branching parameters of neurons grown on gels of different stiffnesses. Together, these data show that the role of substrate rigidity is independent of cell density in shaping the dendritic arbor.

The effect of substrate stiffness and cell number on glutamate concentration

Glutamate is a neurotransmitter that reduces dendrite outgrowth and causes dendrite regression (42). At the synaptic cleft, astrocytes are responsible for the uptake of glutamate (43,44). While there was no difference in the ratio of the number of astrocytes to the number of neurons on soft gels and stiff gels regardless of initial plating density and final cell number, it is possible that there glutamate uptake by astrocytes among these different conditions may differ. Thus, we assessed the amount of global glutamate in the media of cultures: 1) plated on soft or stiff gels with increasing initial cell densities, 2) plated at equivalent initial plating densities on soft and stiff gels, and 3) plated on soft and stiff gels that had equivalent final cell numbers with different or equivalent inital plating densities.

The global glutamate concentration of the media from primary mixed hippocampal cultures plated on gels was measured. Glutamate concentration ranged from approximately 100–300 μM (Figure S4). Data from each set of experiments were normalized to media from cultures plated on soft gels plated at 50,000 cells/cm^2 and averaged for each trial as denoted by the solid horizontal line. The amount of glutamate increased at the highest plating density for cultures on soft or stiff gels (Figure 8 A). In addition, the amount of glutamate measured between cultures plated on soft gels and stiff gels that had equivalent initial plating densities did not change (Figure 8 B). There were also no differences observed in the glutamate concentrations between cultures grown on soft and stiff gels that had equivalent final cell numbers but different initial plating densities, i.e. cells on soft gels plated at 100,000 cells/cm^2 compared to cells on stiff gels plated at 50,000 cells/cm^2 (Figure 8 A, inset). Thus, global glutamate concentrations may not be not responsible for the differences in branching parameters seen for soft and stiff gels but may be responsible for the decreased branching of neurons plated at 100,000 cells/cm^2 on soft and stiff gels.

DISCUSSION

Disease and injury can affect the stiffness of the brain. On a global level, when injury occurs, scarring or intracranial pressure can cause an increase in stiffness (45–49). On a cellular level, injury to astrocytes causes a decrease in astrocyte stiffness (50). Moreover, in MS patients, brain stiffness decreases due to tissue degradation (51). In this study, the stiffness of the soft gel (1kPa) is equivalent to the stiffness of the brain (12) and the stiff gels (7kPa) represent a

disease or injury state. We observed that increasing substrate stiffness (1 kPa vs. 7 kPa) affects dendrite branching in cultured hippocampal neurons.

In the current study, we used primary mixed cultures of hippocampal cells plated on polyacrylamide gels to examine the role that substrate stiffness plays in controlling the chemical, cellular, and mechanical factors that affect dendrite arborization. We looked specifically at whether differences in dendrite branching observed in cell cultures grown on substrates with a range of rigidities are independent of the changes in cell number and astrocytes/neuron ratio caused by the substrates themselves. We observed that there are two pathways by which substrate stiffness exerts its affects on neuronal morphology (Figure 9): 1) an indirect pathway, which is mediated through substrate stiffness-driven changes in the cell number found on the surfaces, and 2) a direct effect, which is independent of the non-neuronal cells found in mixed cultures.

We observed that substrate stiffness affects cell number and type found on the substrates. We found that as stiffness increased, the number of neurons increased at both early time points (24 and 48 hours after plating) and later time points (12 DIV). The early onset and long duration of this trend suggest that the increase in the cell number found on the substrates is due to the attachment of cells to the gels at the time of plating rather than differential cell death or separation from the gels. Because neurons are postmitotic, the increase in the number of neurons cannot be due to cell proliferation. Similarly, we found that as substrate stiffness increased, the number of mature astrocytes increased. While the number of cells found on substrates is sensitive to both initial plating density and substrate stiffness, we found that the ratio of astrocytes to neurons was unaffected by these same conditions. This indicates that the culture composition does not change appreciably, despite the changing number of cells on the surfaces.

Potential mechanisms by which substrate stiffness alters dendrite branching Integrins

The mechanism by which substrate stiffness mediates changes in neuronal morphology in mixed culture is the subject on ongoing debate. There are multiple factors that may play roles in determining changes in neuronal morphology occurring on substrates with different mechanical properties. The final arbor is likely to be the product of the sensitization of the neuron to different activation cues. For example, integrin activation by the substrate may play a role in the differences we see in soft (1 kPa) and hard (7 kPa) gels. Integrins are heterodimer adhesion molecules that are involved in cell-cell and cell-extracellular matrix interactions. Integrin-mediated adhesion increases neurite branching dynamics (52). Integrins show an increase in expression in neurons grown on stiffer substrates (26). Thus, higher expression of integrins and higher integrin-mediated adhesion on stiff gels may contribute to increased dendrite branching. To test this theory, future studies will address the role of integrins and other signaling systems in shaping the dendritic arbors of hippocampal neurons grown on substrates of different rigidities.

Astrocytes

Another way in which stiffness may affect dendritiogenesis is through differential adhesion of astrocytes. Astrocytes not only play key roles in regulating neurite outgrowth by providing neurotropic cues and support (53,54), but they are also responsible for the uptake of glutamate (43,44) at the synaptic cleft. Changes in the number of astrocytes may therefore alter global levels of glutamate. Similarly, neuronal number is increased on the stiff gels, which may result in the increased release of glutamate. Glutamate reduces dendrite outgrowth and causes dendrite regression (42). To elucidate the role the cell-mediated production and uptake of glutamate may play in our system, we examined the global levels of glutamate in cultures grown at equivalent initial plating densities on both soft and stiff substrates as well as for

cultures with equivalent final cell numbers on both soft and stiff substrates. Global glutamate did not change significantly between cultures plated on soft and stiff substrates for cultures with matched initial cell density or for cultures with matched final cell numbers. However, the amount of global glutamate increased significantly at the highest initial plating density for cultures plated on both soft and stiff gels. This could be a result of higher neuronal cell density, and thus, more glutamate release.

Glutamate

The physiological amount of glutamate in the brain is under debate. In the brain, ambient glutamate is 0.6 μM (55,56). However, other groups have reported ambient glutamate to range between 1–4 μM *in vivo* (57–59). In hippocampal slices, ambient glutamate concentrations are 0.025 μM (60). Glutamate concentrations in the synaptic cleft are between 160 and 190 μM (61,62). Intracellular glutamate concentrations are 10 mM in the brain (63). The amount of glutamate in our primary mixed cultures ranged from approximately 100–300 μM, which is in the range of physiological values for the synaptic cleft. Since this concentration of glutamate is below 1 mM. which is considered to elicit the maximal effect of neurotoxicity in dissociated cultures (64,65), we believe that our cultures are not compromised by glutamate-induced toxicity.

Global glutamate concentration may be only one of several mechanisms by which substrate stiffness modulates neuronal morphology. Cell-cell interactions are complex, and numerous studies have shown that interactions between neurons and glia influence dendrite branching (66–68). Specifically, one study by our group has shown that the interaction between neurons and glia plays a significant role in determining dendrite branching patterns in neurons plated on hydrogels (14). However, our present finding that the ratio of astrocytes to neurons does not change significantly between soft and stiff substrates or over the range of seeding densities examined supports the theory that these interactions may not be significantly changed in any of our experimental conditions.

Cell Density vs. Stiffness

Importantly, our results indicate that cell density does indeed play a role in regulating dendrite branching, but this role is secondary to the role of substrate stiffness. In both soft and stiff substrates, the number of astrocytes and neurons increased as initial plating density was increased. On soft substrates, however, none of the measures of branching changed in response to the increased cell number, while on stiff substrates, the number of dendrites decreased with increasing cell number. Similarly, our Sholl analysis indicated a significant density-dependent change in proximal branching on the stiff substrates while no change was present on the soft substrates. While the number of branch points did not change, increased higher order dendrites (i.e., tertiary and quaternary) may have obscured proximal changes. Thus, while density plays a role in regulating branching, the effects of stiffness dominates over the effects of cell density during dendrite arborization.

Our results showed that dendrite morphology is also affected by substrate stiffness directly, even in the absence of a change in final cell number or glutamate concentration. At equivalent initial plating densities, neurons plated on soft gels always had fewer dendrites and branches than those plated on stiff gels. More importantly, when cultures grown on soft and stiff substrates are matched for final cell number, neurons grown on stiff substrates showed an increase in every measure of branching used. Also in this case, these changes in neuronal morphology occurred when culture conditions, such as final cell number, astrocyte/neuron ratio, and global glutamate concentration, were not significantly changed between substrates, leaving substrate stiffness as the only variable. We conclude that the effects of substrate

stiffness on neuronal morphology are not entirely a product of the final numbers of neurons and astrocytes.

The literature regarding the effects of substrate stiffness on neuronal morphology is full of conflicting data, with which this report either corroborates or contradicts in different regards. In contrast to our data, Georges *et al.* showed decreased neuronal adhesion when cells are plated on stiffer substrates versus softer substrates (12), and other groups have shown that neurons plated on softer substrates have more dendrite branches than those grown on stiffer substrates (14,69). However, another study by our group demonstrated that as substrate stiffness increases, the number of neurons in mixed cultures that attach to hydrogels increases (13). Moreover, our laboratory also reported that only pure neuronal or pure glial cultures, but not mixed cultures, showed an increase in cellular adhesion and growth when stiffness increased (14), indicating that the cellular interplay in mixed cultures is complex. These discrepancies can be due to experimental differences in initial plating density, cell types, culture composition, hydrogel rigidities, and culture ages.

Our data support previously published reports showing that neurite outgrowth increases when neurons are plated on substrates of increasing stiffness, although the stiffness range examined was different than that used in this study (13,41). However, our studies are the first to report the separate effects of substrate stiffness, mediated through direct and cell density-dependent pathways, on dendrite branching.

Supplementary Material

Refer to Web version on PubMed Central for supplementary material.

Acknowledgments

This work was funded by National Science Foundation IBN-0548543, March of Dimes 1-FY08-464, New Jersey Commission Brain Injury Research, BIR2 #08.004, and American Heart Association Grant-In-Aid 0555801T . MLP was supported by IGERT Program on Biointerfaces NSF grant DGE-0333196 and a Louis Bevier Dissertation Fellowship. CGL was supported by NIH Biotechnology Training Grant T32 GM008339-20 and New Jersey Commission on Spinal Cord Injury Predoctoral Fellowship #08-2941-SCR-E-0. We would also like to thank Drs. Noshir Langrana and Uday Chippada for help with mechanical testing.

REFERENCES

1. Jan YN, Jan LY. The control of dendrite development. Neuron 2003;40:229–242. [PubMed: 14556706]
2. Spruston N. Pyramidal neurons: Dendritic structure and synaptic integration. Nat. Rev. Neurosci 2008;9:206–221. [PubMed: 18270515]
3. Landgraf M, Evers JF. Control of dendritic diversity. Curr. Opin. Cell Biol 2005;17:690–696. [PubMed: 16226445]
4. Anderton BH, Callahan L, Coleman P, Davies P, Flood D, Jicha GA, Ohm T, Weaver C. Dendritic changes in alzheimer's disease and factors that may underlie these changes. Prog. Neurobiol 1998;55:595–609. [PubMed: 9670220]
5. Harrison PJ. The neuropathology of schizophrenia. A critical review of the data and their interpretation. Brain 1999;122(Pt 4):593–624. [PubMed: 10219775]
6. Zoghbi HY. Postnatal neurodevelopmental disorders: Meeting at the synapse? Science 2003;302:826–830. [PubMed: 14593168]
7. Dotti CG, Sullivan CA, Banker GA. The establishment of polarity by hippocampal neurons in culture. J. Neurosci 1988;8:1454–1468. [PubMed: 3282038]
8. Akum BF, Chen M, Gunderson SI, Riefler GM, Scerri-Hansen MM, Firestein BL. Cypin regulates dendrite patterning in hippocampal neurons by promoting microtubule assembly. Nat. Neurosci 2004;7:145–152. [PubMed: 14730308]

9. Georges PC, Hadzimichalis NM, Sweet ES, Firestein BL. The yin-yang of dendrite morphology: Unity of actin and microtubules. Mol. Neurobiol 2008;38:270–284. [PubMed: 18987787]
10. Vessey JP, Karra D. More than just synaptic building blocks: Scaffolding proteins of the post-synaptic density regulate dendritic patterning. J. Neurochem 2007;102:324–332. [PubMed: 17596209]
11. Charych EI, Akum BF, Goldberg JS, Jornsten RJ, Rongo C, Zheng JQ, Firestein BL. Activity-independent regulation of dendrite patterning by postsynaptic density protein psd-95. J. Neurosci 2006;26:10164–10176. [PubMed: 17021172]
12. Georges PC, Miller WJ, Meaney DF, Sawyer ES, Janmey PA. Matrices with compliance comparable to that of brain tissue select neuronal over glial growth in mixed cortical cultures. Biophys. J 2006;90:3012–3018. [PubMed: 16461391]
13. Jiang FX, Yurke B, Firestein BL, Langrana NA. Neurite outgrowth on a DNA crosslinked hydrogel with tunable stiffnesses. Ann. of Biomed. Eng 2008;36:1565–1579. [PubMed: 18618260]
14. Jiang X, Georges PC, Li B, Du Y, Kutzing MK, Previtera ML, Langrana NA, Firestein BL. Cell growth in response to mechanical stiffness is affected by neuron-astroglia interactions. The Open Neuroscience Journal 2007;1:7–14.
15. Cove J, Blinder P, Abi-Jaoude E, Lafreniere-Roula M, Devroye L, Baranes D. Growth of neurites toward neurite- neurite contact sites increases synaptic clustering and secretion and is regulated by synaptic activity. Cereb. Cortex 2006;16:83–92. [PubMed: 15858165]
16. Horwitz B. Neuronal plasticity: How changes in dendritic architecture can affect the spread of postsynaptic potentials. Brain Res 1981;224:412–418. [PubMed: 7284849]
17. Cove J, Blinder P, Baranes D. Contacts among non-sister dendritic branches at bifurcations shape neighboring dendrites and pattern their synaptic inputs. Brain Res 2009;1251:30–41. [PubMed: 19046952]
18. Komiyama T, Luo L. Development of wiring specificity in the olfactory system. Curr. Opin. Neurobiol 2006;16:67–73. [PubMed: 16377177]
19. Urbanska M, Blazejczyk M, Jaworski J. Molecular basis of dendritic arborization. Acta. Neurobiol. Exp. (Wars) 2008;68:264–288. [PubMed: 18511961]
20. Liagkouras I, Michaloudi H, Batzios C, Psaroulis D, Georgiadis M, Kunzle H, Papadopoulos GC. Pyramidal neurons in the septal and temporal ca1 field of the human and hedgehog tenrec hippocampus. Brain Res 2008;1218:35–46. [PubMed: 18511020]
21. McAllister AK. Cellular and molecular mechanisms of dendrite growth. Cereb. Cortex 2000;10:963–973. [PubMed: 11007547]
22. McAllister AK, Lo DC, Katz LC. Neurotrophins regulate dendritic growth in developing visual cortex. Neuron 1995;15:791–803. [PubMed: 7576629]
23. Vaughn JE. Fine structure of synaptogenesis in the vertebrate central nervous system. Synapse 1989;3:255–285. [PubMed: 2655146]
24. Bartlett WP, Banker GA. An electron microscopic study of the development of axons and dendrites by hippocampal neurons in culture. Ii. Synaptic relationships. J. Neurosci 1984;4:1954–1965. [PubMed: 6470763]
25. Bartlett WP, Banker GA. An electron microscopic study of the development of axons and dendrites by hippocampal neurons in culture. I. Cells which develop without intercellular contacts. J. Neurosci 1984;4:1944–1953. [PubMed: 6470762]
26. Yeung T, Georges PC, Flanagan LA, Marg B, Ortiz M, Funaki M, Zahir N, Ming W, Weaver V, Janmey PA. Effects of substrate stiffness on cell morphology, cytoskeletal structure, and adhesion. Cell. Motil. Cytoskeleton 2005;60:24–34. [PubMed: 15573414]
27. Pelham RJ, Wang YL. Cell locomotion and focal adhesions are regulated by the mechanical properties of the substrate. Biol. Bull 1998;194:348–350. [PubMed: 11536880]
28. Georges PC, Janmey PA. Cell type-specific response to growth on soft materials. J. Appl. Physiol 2005;98:1547–1553. [PubMed: 15772065]
29. Firestein BL, Brenman JE, Aoki C, Sanchez-Perez AM, El-Husseini AE, Bredt DS. Cypin: A cytosolic regulator of psd-95 postsynaptic targeting. Neuron 1999;24:659–672. [PubMed: 10595517]
30. Nikolic M, Dudek H, Kwon YT, Ramos YF, Tsai LH. The cdk5/p35 kinase is essential for neurite outgrowth during neuronal differentiation. Genes Dev 1996;10:816–825. [PubMed: 8846918]

31. Bonni A, Ginty DD, Dudek H, Greenberg ME. Serine 133-phosphorylated creb induces transcription via a cooperative mechanism that may confer specificity to neurotrophin signals. Mol. Cell. Neurosci 1995;6:168–183. [PubMed: 7551568]
32. Dudek H, Datta SR, Franke TF, Birnbaum MJ, Yao R, Cooper GM, Segal RA, Kaplan DR, Greenberg ME. Regulation of neuronal survival by the serine-threonine protein kinase akt. Science 1997;275:661–665. [PubMed: 9005851]
33. Xia Z, Dudek H, Miranti CK, Greenberg ME. Calcium influx via the nmda receptor induces immediate early gene transcription by a map kinase/erk-dependent mechanism. J. Neurosci 1996;16:5425–5436. [PubMed: 8757255]
34. Meijering E, Jacob M, Sarria JC, Steiner P, Hirling H, Unser M. Design and validation of a tool for neurite tracing and analysis in fluorescence microscopy images. Cytometry A 2004;58:167–176. [PubMed: 15057970]
35. Vallotton P, Lagerstrom R, Sun C, Buckley M, Wang D, De Silva M, Tan SS, Gunnersen JM. Automated analysis of neurite branching in cultured cortical neurons using hca-vision. Cytometry A 2007;71:889–895. [PubMed: 17868085]
36. Ascoli GA, Krichmar JL, Nasuto SJ, Senft SL. Generation, description and storage of dendritic morphology data. Philos. Trans. R. Soc. Lond. B Bio.l Sci 2001;356:1131–1145. [PubMed: 11545695]
37. Cannon RC, Turner DA, Pyapali GK, Wheal HV. An on-line archive of reconstructed hippocampal neurons. J. Neurosci. Methods 1998;84:49–54. [PubMed: 9821633]
38. Wearne SL, Rodriguez A, Ehlenberger DB, Rocher AB, Henderson SC, Hof PR. New techniques for imaging, digitization and analysis of three-dimensional neural morphology on multiple scales. Neuroscience 2005;136:661–680. [PubMed: 16344143]
39. Carrel D, Du Y, Komlos D, Hadzimichalis NM, Kwon M, Wang B, Brzustowicz LM, Firestein BL. Nos1ap regulates dendrite patterning of hippocampal neurons through a carboxypeptidase e-mediated pathway. J. Neurosci 2009;29:8248–8258. [PubMed: 19553464]
40. Chen M, Lucas KG, Akum BF, Balasingam G, Stawicki TM, Provost JM, Riefler GM, Jornsten RJ, Firestein BL. A novel role for snapin in dendrite patterning: Interaction with cypin. Mol. Biol. Cell 2005;16:5103–5114. [PubMed: 16120643]
41. Leach JB, Brown XQ, Jacot JG, Dimilla PA, Wong JY. Neurite outgrowth and branching of pc12 cells on very soft substrates sharply decreases below a threshold of substrate rigidity. J. Neural. Eng 2007;4:26–34. [PubMed: 17409477]
42. Mattson MP, Dou P, Kater SB. Outgrowth-regulating actions of glutamate in isolated hippocampal pyramidal neurons. J. Neurosci 1988;8:2087–2100. [PubMed: 2898515]
43. Rothstein JD, Martin L, Levey AI, Dykes-Hoberg M, Jin L, Wu D, Nash N, Kuncl RW. Localization of neuronal and glial glutamate transporters. Neuron 1994;13:713–725. [PubMed: 7917301]
44. Danbolt NC. Glutamate uptake. Prog. Neurobiol 2001;65:1–105. [PubMed: 11369436]
45. Marmarou A, Maset AL, Ward JD, Choi S, Brooks D, Lutz HA, Moulton RJ, Muizelaar JP, DeSalles A, Young HF. Contribution of csf and vascular factors to elevation of icp in severely head-injured patients. J. Neurosurg 1987;66:883–890. [PubMed: 3572518]
46. Hertegard S, Cedervall J, Svensson B, Forsberg K, Maurer FH, Vidovska D, Olivius P, Ahrlund-Richter L, Le Blanc K. Viscoelastic and histologic properties in scarred rabbit vocal folds after mesenchymal stem cell injection. Laryngoscope 2006;116:1248–1254. [PubMed: 16826069]
47. Hertegard S, Dahlqvist A, Goodyer E. Viscoelastic measurements after vocal fold scarring in rabbits--short-term results after hyaluronan injection. Acta Otolaryngol 2006;126:758–763. [PubMed: 16803717]
48. Manwaring P, Wichern D, Manwaring M, Manwaring J, Manwaring K. A signal analysis algorithm for determining brain compliance non-invasively. Conf. Proc. IEEE Eng. Med. Biol. Soc 2004;1:353–356. [PubMed: 17271683]
49. Corr DT, Gallant-Behm CL, Shrive NG, Hart DA. Biomechanical behavior of scar tissue and uninjured skin in a porcine model. Wound Repair Regen 2009;17:250–259. [PubMed: 19320894]
50. Miller WJ, Leventhal I, Scarsella D, Haydon PG, Janmey P, Meaney DF. Mechanically induced reactive gliosis causes atp-mediated alterations in astrocyte stiffness. J. Neurotrauma 2009;26:789–797. [PubMed: 19331521]

51. Wuerfel J, Paul F, Beierbach B, Hamhaber U, Klatt D, Papazoglou S, Zipp F, Martus P, Braun J, Sack I. Mr-elastography reveals degradation of tissue integrity in multiple sclerosis. Neuroimage 2009;49:2520–2525. [PubMed: 19539039]
52. Moresco EM, Donaldson S, Williamson A, Koleske AJ. Integrin-mediated dendrite branch maintenance requires abelson (abl) family kinases. J. Neurosci 2005;25:6105–6118. [PubMed: 15987940]
53. Pierret P, Quenneville N, Vandaele S, Abbaszadeh R, Lanctot C, Crine P, Doucet G. Trophic and tropic effects of striatal astrocytes on cografted mesencephalic dopamine neurons and their axons. J. Neurosci. Res 1998;51:23–40. [PubMed: 9452306]
54. Gomes FC, Spohr TC, Martinez R, Moura Neto V. Cross-talk between neurons and glia: Highlights on soluble factors. Braz. J .Med. Biol. Res 2001;34:611–620. [PubMed: 11323747]
55. Benveniste H, Drejer J, Schousboe A, Diemer NH. Elevation of the extracellular concentrations of glutamate and aspartate in rat hippocampus during transient cerebral ischemia monitored by intracerebral microdialysis. J. Neurochem 1984;43:1369–1374. [PubMed: 6149259]
56. Bouvier M, Szatkowski M, Amato A, Attwell D. The glial cell glutamate uptake carrier countertransports ph-changing anions. Nature 1992;360:471–474. [PubMed: 1448171]
57. Nyitrai G, Kekesi KA, Juhasz G. Extracellular level of gaba and glu: In vivo microdialysis-hplc measurements. Curr. Top. Med. Chem 2006;6:935–940. [PubMed: 16787267]
58. Baker DA, Xi ZX, Shen H, Swanson CJ, Kalivas PW. The origin and neuronal function of in vivo nonsynaptic glutamate. J. Neurosci 2002;22:9134–9141. [PubMed: 12388621]
59. Lerma J, Herranz AS, Herreras O, Abraira V, Martin del Rio R. In vivo determination of extracellular concentration of amino acids in the rat hippocampus. A method based on brain dialysis and computerized analysis. Brain Res 1986;384:145–155. [PubMed: 3790989]
60. Herman MA, Jahr CE. Extracellular glutamate concentration in hippocampal slice. J. Neurosci 2007;27:9736–9741. [PubMed: 17804634]
61. Dzubay JA, Jahr CE. The concentration of synaptically released glutamate outside of the climbing fiber-purkinje cell synaptic cleft. J. Neurosci 1999;19:5265–5274. [PubMed: 10377338]
62. Timmerman W, Westerink BH. Brain microdialysis of gaba and glutamate: What does it signify? Synapse 1997;27:242–261. [PubMed: 9329159]
63. Kvamme E, Schousboe A, Hertz L, Torgner IA, Svenneby G. Developmental change of endogenous glutamate and gamma-glutamyl transferase in cultured cerebral cortical interneurons and cerebellar granule cells, and in mouse cerebral cortex and cerebellum in vivo. Neurochem. Res 1985;10:993–1008. [PubMed: 2864647]
64. Rosenberg PA, Amin S, Leitner M. Glutamate uptake disguises neurotoxic potency of glutamate agonists in cerebral cortex in dissociated cell culture. J. Neurosci 1992;12:56–61. [PubMed: 1345946]
65. Choi DW, Maulucci-Gedde M, Kriegstein AR. Glutamate neurotoxicity in cortical cell culture. J. Neurosci 1987;7:357–368. [PubMed: 2880937]
66. Yamamoto M, Ueda R, Takahashi K, Saigo K, Uemura T. Control of axonal sprouting and dendrite branching by the nrg-ank complex at the neuron-glia interface. Curr. Biol 2006;16:1678–1683. [PubMed: 16920632]
67. Tropea M, Johnson MI, Higgins D. Glial cells promote dendritic development in rat sympathetic neurons in vitro. Glia 1988;1:380–392. [PubMed: 2976398]
68. Higgins D, Burack M, Lein P, Banker G. Mechanisms of neuronal polarity. Curr. Opin. Neurobiol 1997;7:599–604. [PubMed: 9384542]
69. Flanagan LA, Ju YE, Marg B, Osterfield M, Janmey PA. Neurite branching on deformable substrates. Neuroreport 2002;13:2411–2415. [PubMed: 12499839]

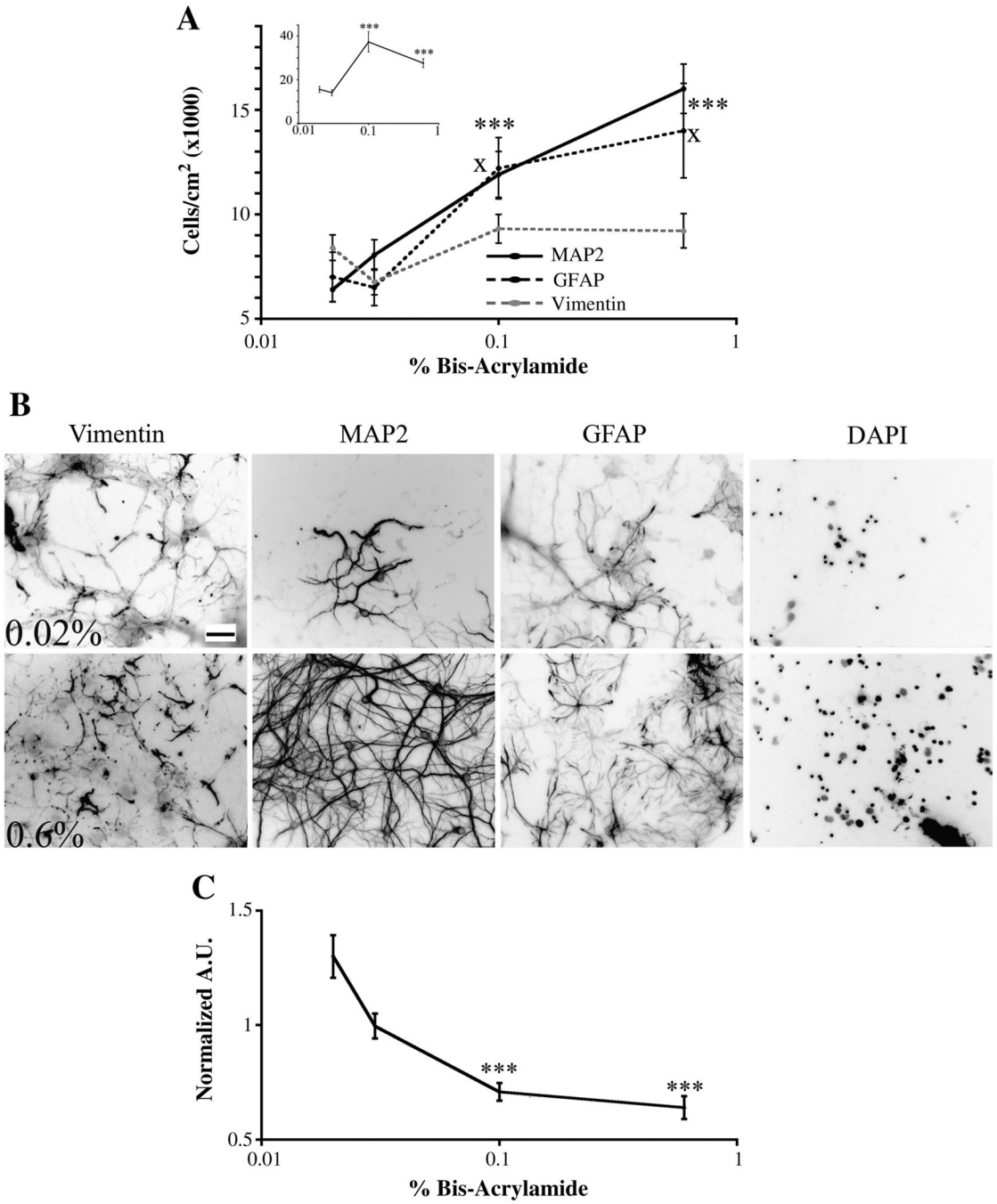

Figure 1.

The number of neurons and astrocytes on gels of varying stiffnesses. (A) The number of neurons and mature astrocytes increases as gel stiffness increased as assessed on 12 DIV. The number of immature astrocytes did not change when the cells were plated on gels of different stiffnesses. Inset, total cell number increased when cells were plated on 0.03% versus 0.1% gels. ***$p<0.001$ for MAP2-positive cells and $^{x}p<0.05$ for GFAP-positive cells determined by Kruskal-Wallis Test followed by Dunn's Multiple Comparison Test compared to 0.02% bis-acrylamide gels. (B) Representative images quantitated in panel A. Scale bar = 50 μm. Numbers of pictures taken for each condition are listed for 0.02, 0.03, 0.1, and 0.6% bis-acrylamide gels, respectively. Vimentin: n=54; 44; 59; 46. MAP2: n=36; 34; 30; 35. GFAP: n=29; 39; 38; 30,

DAPI: n-86; 87; 94; 86. (C) PDL retained decreased as gel stiffness increased. Data normalized to 0.02% bis-acrylamide gels. Arbitrary units (A.U.). ***$p<0.001$ determined by Kruskal-Wallis Test followed by Dunn's Multiple Comparison Test compared to 0.02% bis-acrylamide gels. Numbers of pictures taken for each condition for PDL are listed for 0.02, 0.03, 0.1, and 0.6% bis-acrylamide gels, respectively: n= 36; 36; 31; 36. Data were averaged across three to seven experiments. All data are represented as mean ± SEM.

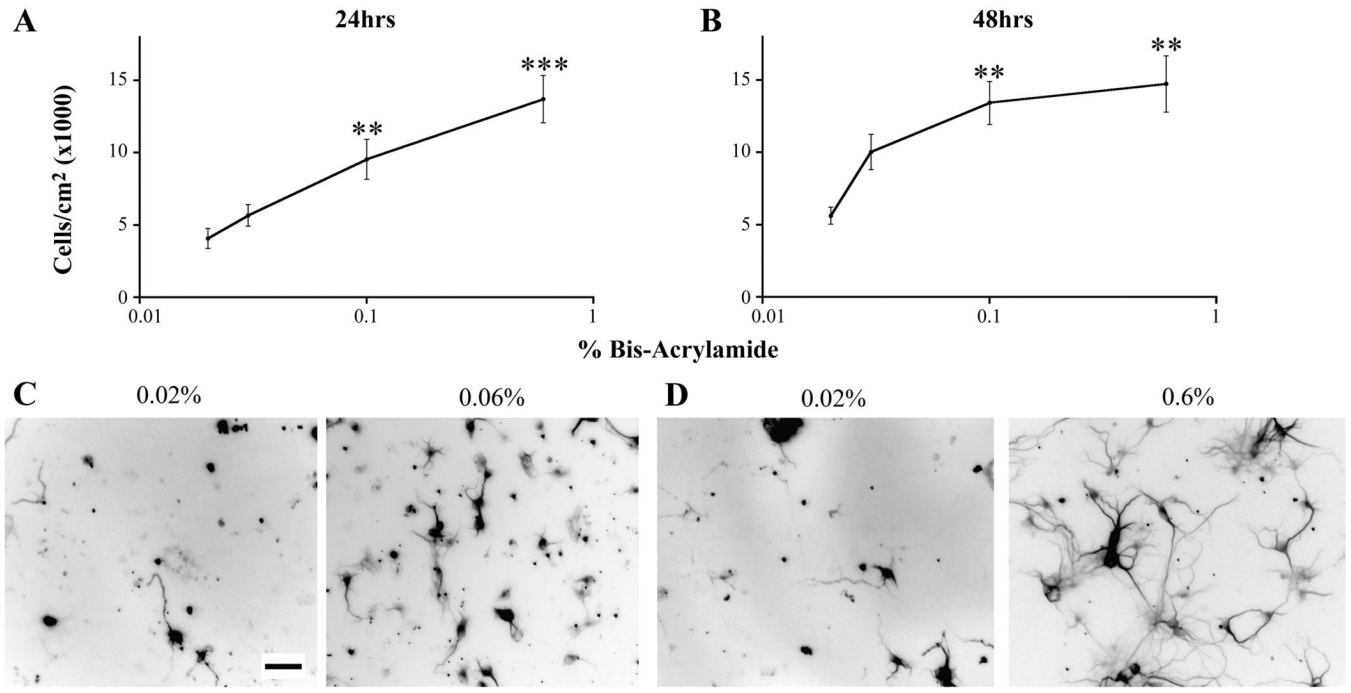

Figure 2.

Differences in cell number early in culture. Cells were plated at an initial density of 60,000 cells/cm^2. (A) The number of neurons was determined 24 hours after plating. **p<0.01 and ***p<0.001 determined by Kruskal-Wallis Test followed by Dunn's Multiple Comparison Test compared to cultures grown on 0.02% bis-acrylamide gels. (B) The number of neurons was determined 48 hours after plating. **p<0.01 determined by Kruskal-Wallis Test followed by Dunn's Multiple Comparison Test compared to cultures grown on 0.02% gels. (C, D) Representative images of neurons cultured on 0.02 and 0.06 % bis-acrylamide gels quantitated in panels A and B. Scale bar = 50 μm. The numbers of pictures taken for each condition are listed for cultures grown on 0.02, 0.03, 0,01, and 0.06% bis-acrylamide gels, respectively. 24 hours: n=30; 55; 56; 55. 48 hours: n=43; 49; 54; 55. Data were averaged across four experiments. All data are represented as mean ± SEM.

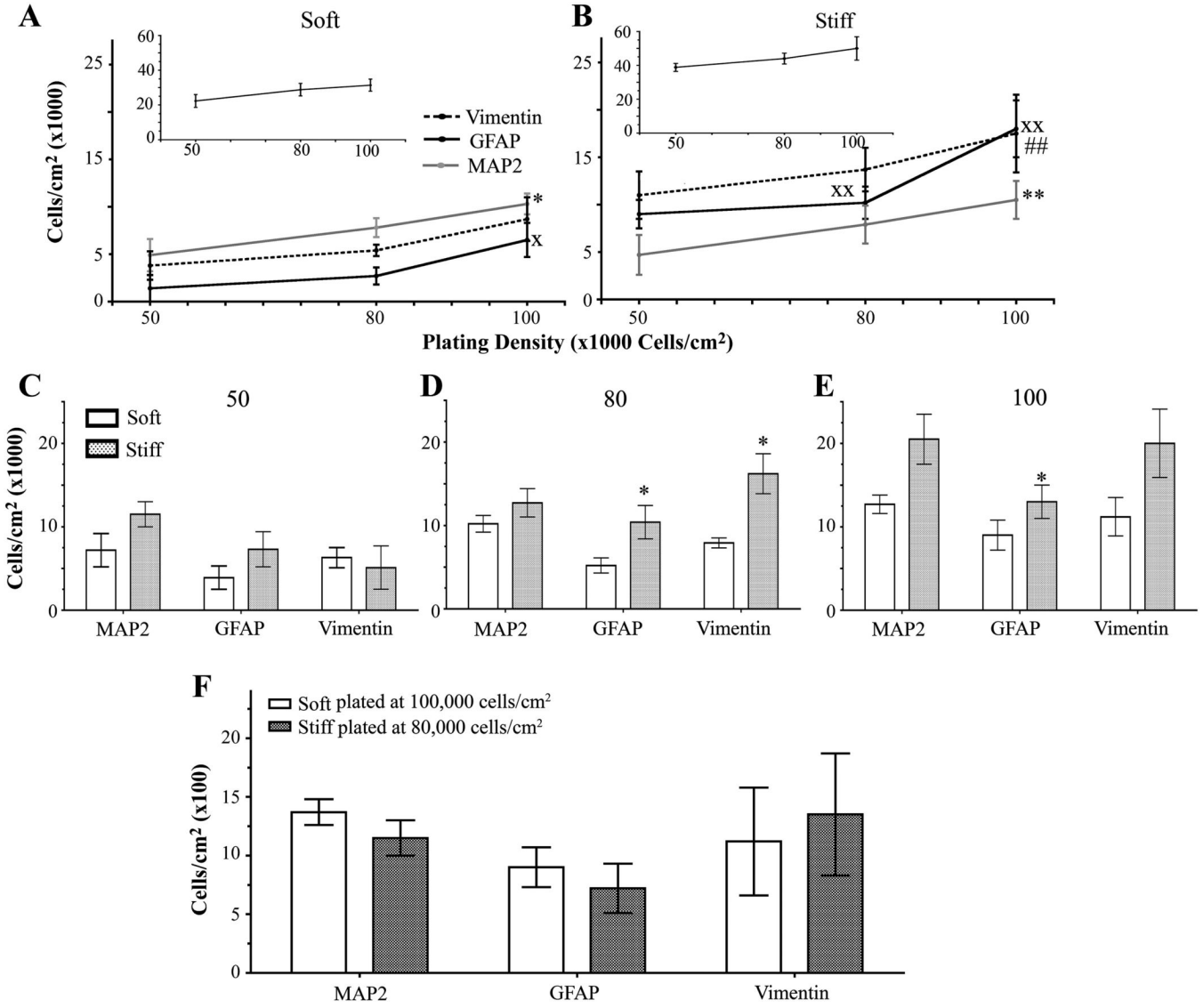

Figure 3.

Cell density changes seen with different substrate stiffnesses and initial plating densities. (A) When grown on soft gels and assessed on 12 DIV, the number of neurons and mature astocytes increased as initial plating density increased. The number of vimentin-positive cells did not change as initial plating density increased. Inset shows that the total number of cells remains unchanged with increased plating density. $^{x}p<0.05$ for GFAP-positive cells determined by one-way ANOVA followed by Dunnett's Multiple Comparison Test compared to 50,000 cells/cm^2. *p<0.05 for MAP2-positive cells determined by repeated one-way ANOVA followed by Dunnett's Multiple Comparison Test compared to 50,000 cells/cm^2. (B) As initial plating density increased, the number of neurons increased and the number of mature astrocytes remained unchanged on stiff gels. Inset shows that the total number of cells remains unchanged with increased plating density. $^{xx}p<0.01$ for GFAP-positive cells determined by repeated one-way ANOVA followed by Dunnett's Multiple Comparison Test compared to 50,000 cells/cm^2. **p<0.01 for MAP2-positive cells determined by repeated one-way ANOVA followed by Dunn's Multiple Comparison Test compared to 50,000 cells/cm^2. $^{\#\#}p<0.01$ for vimentin-positive cells determined by repeated one-way ANOVA followed by Dunn's Multiple

Comparison Test compared to 50,000 cells/cm^2 (C) No differences in the number of MAP2-, GFAP-, and vimentin-positive cells were observed between soft and stiff substrates when cells were initially plated at 50,000 cells/cm^2. (D) Stiff substrates have an increased number of MAP2- and GFAP-positive cells when plated at an initial density of 80,000 cells/cm^2 when compared to soft substrates. *$p<0.05$ determined by Mann-Whitney Test. (E) Stiff gels have an increased number of GFAP-positive cells when plated at a initial density of 100,000 cells/cm^2 when compared to soft gels. *$p<0.05$ determined by paired t-test. (F) Mixed cultures plated on soft gels at 100,000 cells/cm^2 or stiff gels at 50,000 cells/cm^2 have the same number of MAP2-, GFAP-, and vimentin-positive cells. Data were combined averages of four to eight experiments. All data are represented as mean ± SEM.

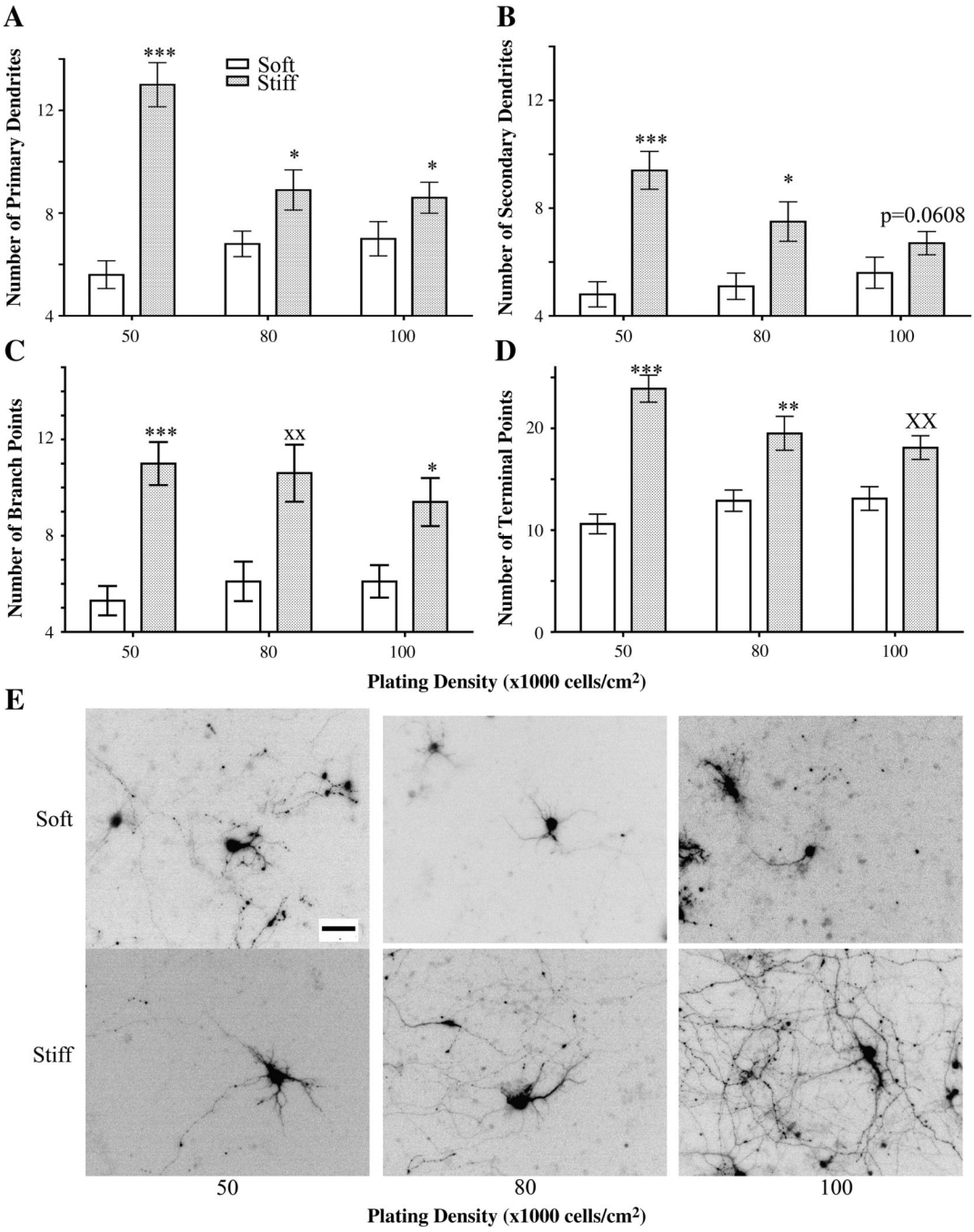

Figure 4.

Dendrite branching patterns of neurons plated at different initial densities and on different substrate rigidities as assessed on 12 DIV. Neurons plated on stiff gels had more primary (A) and secondary (B) dendrites than those plated on soft gels at the same initial cell density. ***$p<0.0001$ and *$p<0.05$ determined by Mann-Whitney Test. (C) Numbers of dendrite branch points increased in neurons plated on stiff gels compared to those plated on soft gels when plated at an initial density of 50,000 cells/cm^2. ***$p<0.0001$ and *$p<0.05$ determined by Mann-Whitney Test. **$p<0.01$ determined by Student's t-test. (D) Numbers of dendrite terminal points increased in neurons plated on stiff gels compared to those grown on soft gels when plated at an initial density of 50,000 cells/cm^2. ***$p<0.0001$ and **$p<0.01$ determined by

Mann-Whitney Test and $^{xx}p<0.01$ determined by Student's t-Test. (E) Representative, inverted images of GFP-expressing neurons quantitated in panels A–E. Data were averaged across four experiments. All data are represented as mean ± SEM. Numbers of cells for each condition are listed for 50,000, 80,000, and 100,000 cells/cm^2, respectively. Soft gels: n= 28; 37; 34. Stiff gels: 35; 30; 33. Scale bar, 50 μm.

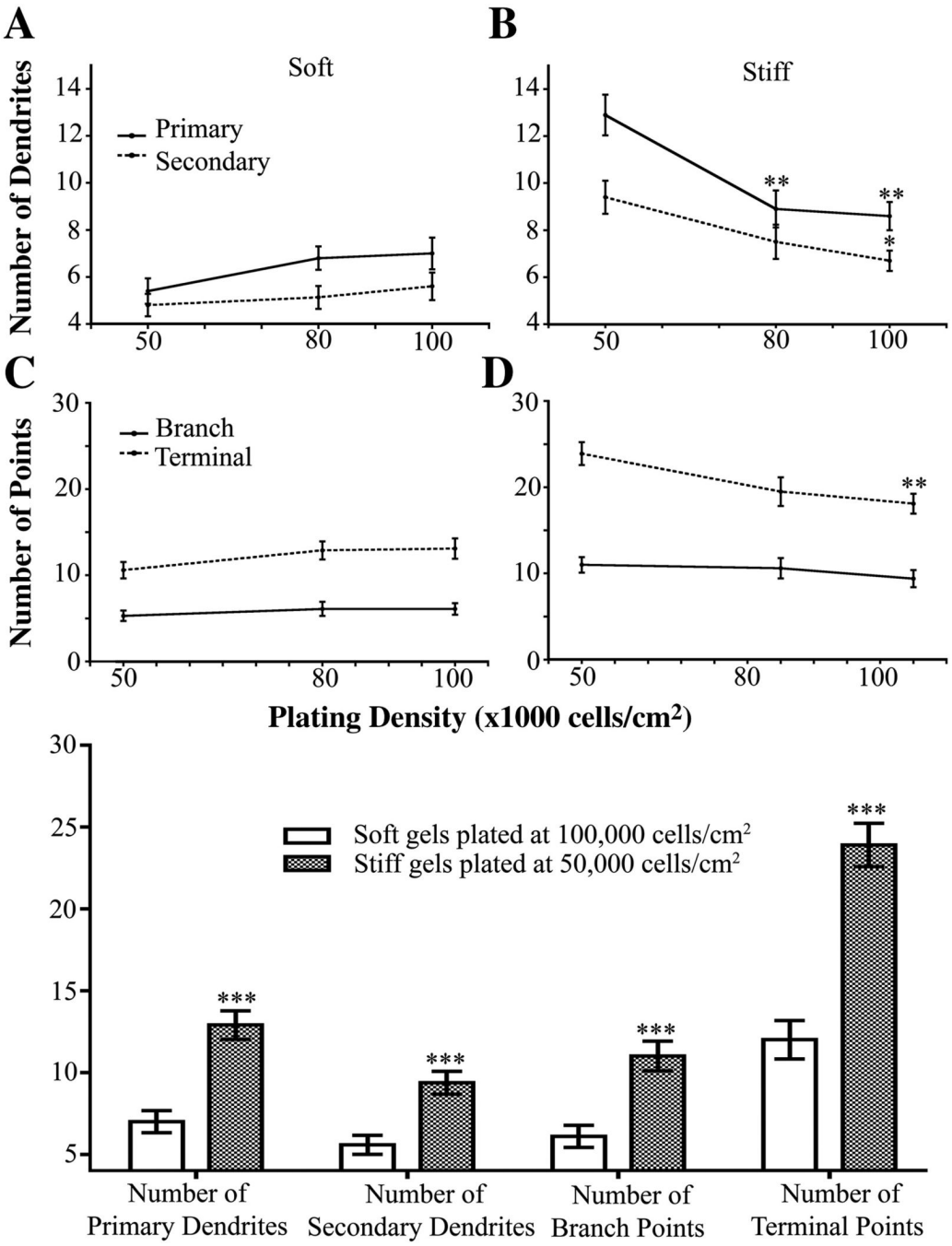

Figure 5.

The number of dendrites is independent of initial plating density for neurons grown on soft gels. (A) Neurons plated on soft gels showed no change in number of primary or secondary dendrites. (B) Neurons plated on stiff gels have less primary and secondary dendrites when plated at higher initial cell densities. **$p<0.01$ for primary dendrite number determined by ANOVA followed by Dunnett's Multiple Comparison Test compared to initial plating density of 50,000 cells/cm^2. *$p<0.05$ for secondary dendrites determined by Kruskal-Wallis Test followed by Dunn's Multiple Comparison Test compared to initial plating density of 50,000 cells/cm^2. (C) Number of dendrite branch and terminal points did not change in neurons plated at increasing cell densities on soft gels. (D) Number of dendrite branch points did not change,

but number of terminal points decreased, in neurons plated at increasing cell densities on stiff gels. **p<0.01 determined by ANOVA followed by Dunnett's Multiple Comparison Test compared to 50,000 cells/cm^2. Data were averaged across four experiments All data are represented as mean ± SEM. Numbers of cells for each condition are listed for 50,000, 80,000, and 100,000 cells/cm^2, respectively. Soft gels: n= 28; 37; 34. Stiff gels: 35; 30; 33.

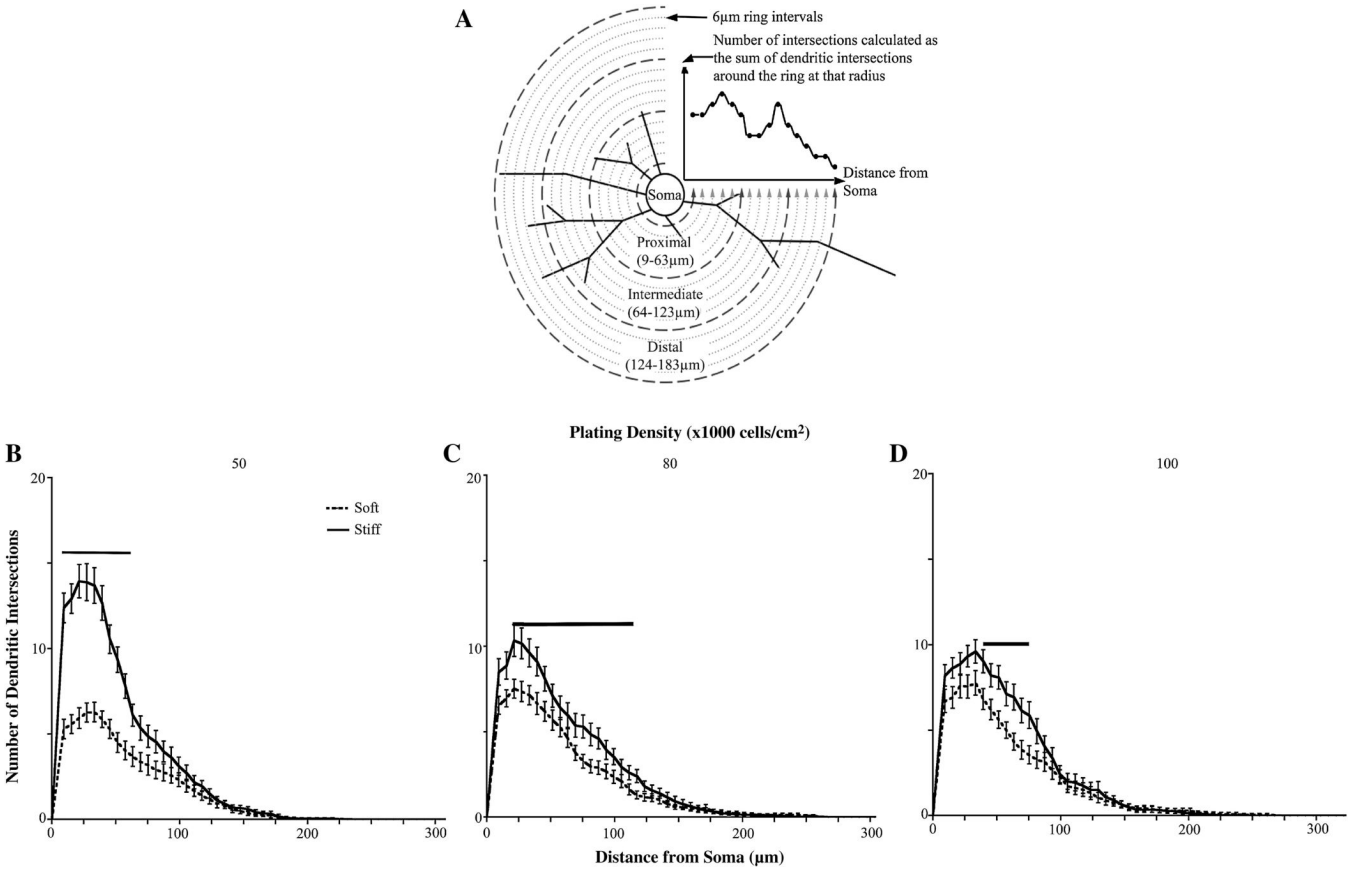

Figure 6.

Sholl analysis of neurons cultured on gels of varying rigidities. (A) Explanation of Sholl analysis. Concentric circles are drawn around the cell body. Dendritic intersections are counted at each circle. Proxmal dendrites are counted within 63 μm from the cell body, intermediate dendrites are counted within 123 μm from the cell body, and distal dendrites are between 123–183 μm from the cell body. (B) Sholl analysis of neurons plated at an initial cell density of 50,000 cells/cm^2 (C) Sholl analysis of neurons plated at an initial cell density of 80,000 cells/cm^2 (D) Sholl analysis of neurons plated at an initial cell density of 100,000 cells/cm^2. For all conditions, neurons showed increased proximal and intermediate branches when cultured on stiff versus soft gels. (See Tables S1–3 for p values). Bars indicate significance with $p<0.05$. Data were averaged across four experiments. All data are represented as mean ± SEM. Numbers of cells for each condition are listed for 50,000, 80,000, and 100,000 cells/cm^2, respectively. Soft gels: n=28; 37; 34. Stiff gels: 35; 30; 33.

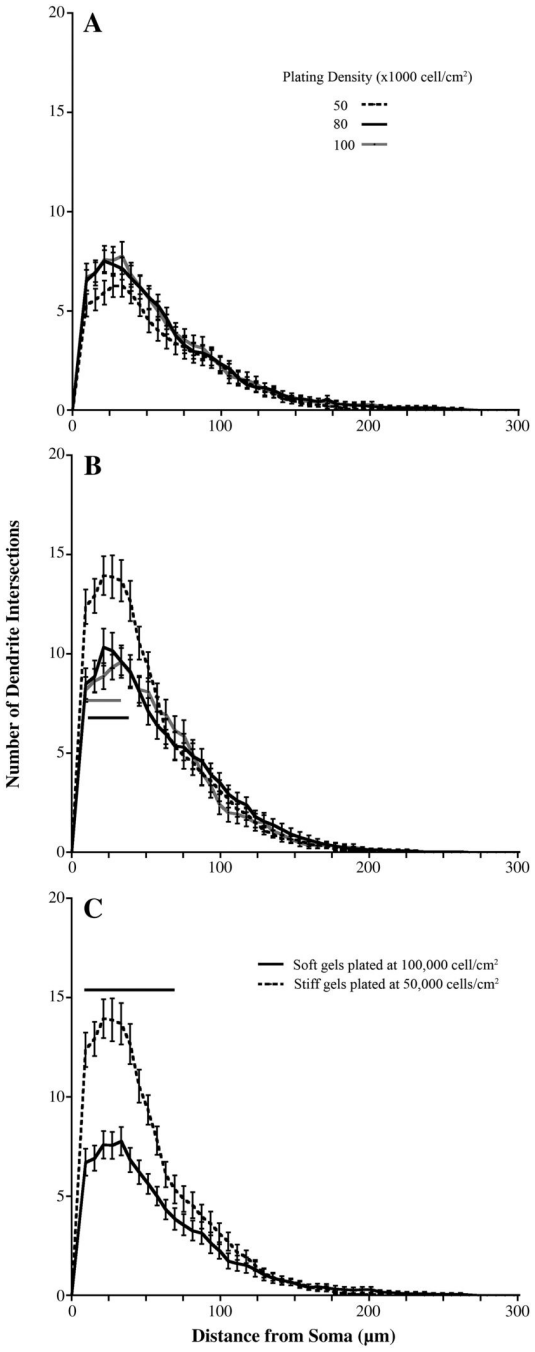

Figure 7.

Sholl analysis of neurons cultured at different initial plating densities. (A) Initial plating density had no effect on dendrites when neurons were cultured on soft gels. (B) When plated at the lowest density (50,000 cells/cm^2), neurons cultured on stiff gels had the most proximal dendrites (See Table S4 for p values). (C) Sholl analysis of neurons cultured on soft and stiff gels with the same final number of cells. (See Table S5 for p values). Bar indicates significance. Data were averaged across four experiments. All data are represented as mean ± SEM. Numbers of cells for each condition are listed for 50,000, 80,000, and 100,000 cells/cm^2, respectively. Soft gels: n= 28; 37; 34. Stiff gels: 35; 30; 33.

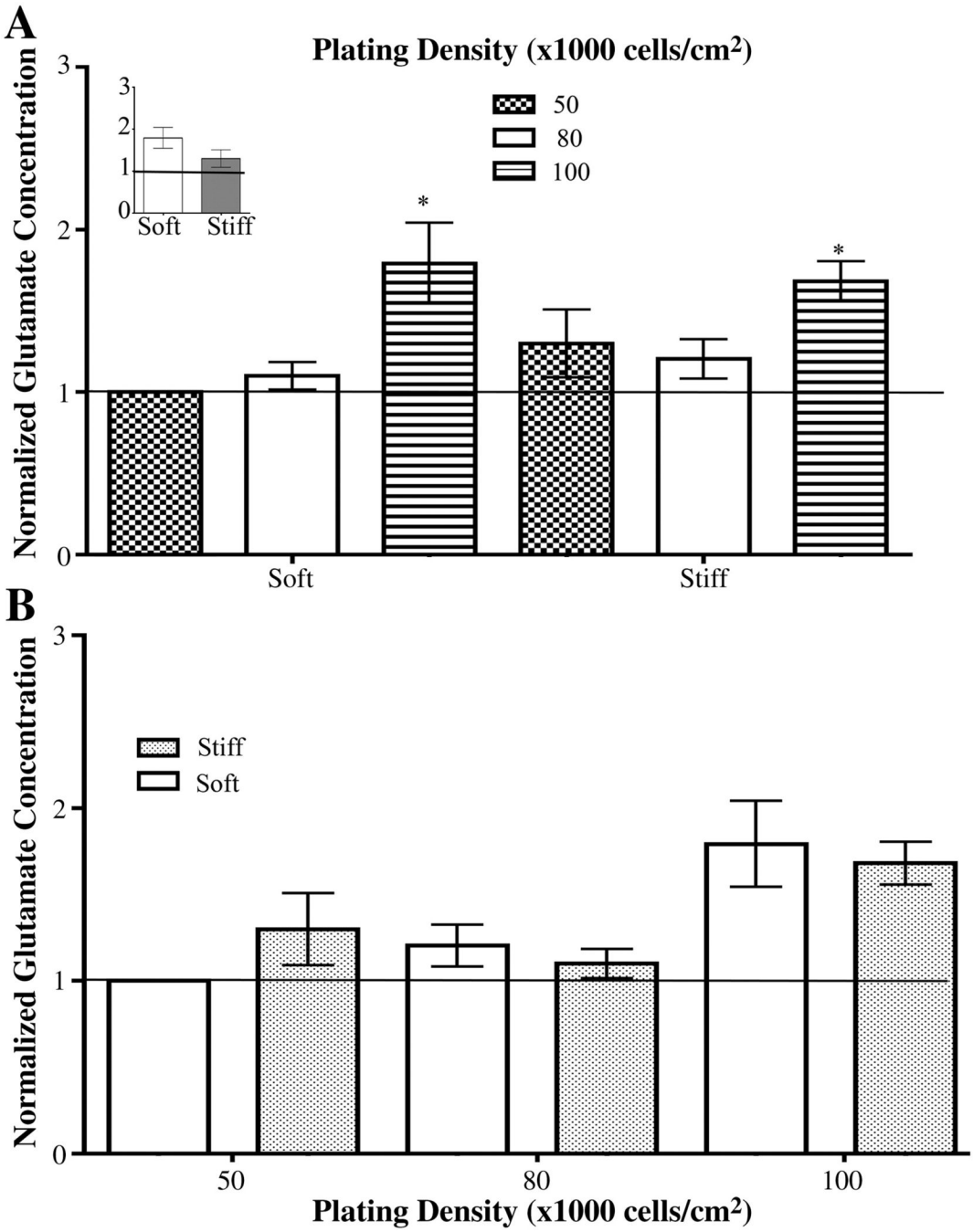

Figure 8.

Glutamate concentrations found in the media of cells cultured under different conditions. (A) Glutamate concentration in the media increased when cells were plated at 100,000 cells/cm^2 on both soft and stiff gels gels. *p<0.05 for soft gels determined by Kruskal-Wallis followed by Dunn's Multiple Comparison Test compared to cells plated at 50,000 cells/cm$^{2\cdot}$. *p<0.05 for stiff gels determined by repeated one-way ANOVA followed by Dunnett's Multiple Comparison Test compared to cells plated at 50,000 cells/cm^2. Glutamate concentration in the media did not change as initial plating density increased. Inset shows that glutamate did not change when cells were plated such that final cell numbers were the same on the soft and stiff gels. (B). Glutamate concentrations were the same in media taken from cultures on soft and

stiff gels with the same initial number of cells. Data were averaged across five experiments. All data are represented as mean ± SEM.

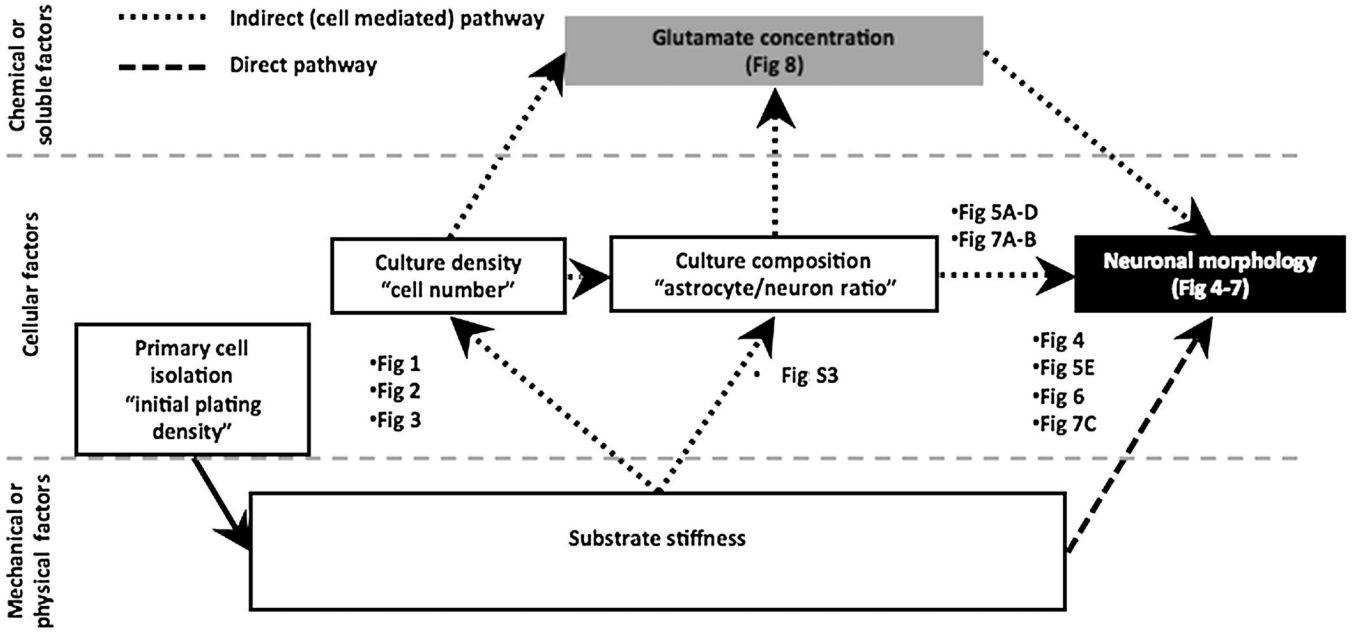

Figure 9.

Schematic showing direct pathway and indirect, cell-mediated pathway by which substrate stiffness affects dendrite morphology. Each step connecting one factor to another factor has been labeled with the figures within this paper elucidating the relationship between the two concepts connected.